

Towards Physically Realizable Adversarial Attacks in Embodied Vision Navigation

Meng Chen¹, Jiawei Tu¹, Chao Qi¹, Yonghao Dang¹, Feng Zhou¹, Wei Wei¹, Jianqin Yin^{1,*}

Abstract—The significant advancements in embodied vision navigation have raised concerns about its susceptibility to adversarial attacks exploiting deep neural networks. Investigating the adversarial robustness of embodied vision navigation is crucial, especially given the threat of 3D physical attacks that could pose risks to human safety. However, existing attack methods for embodied vision navigation often lack physical feasibility due to challenges in transferring digital perturbations into the physical world. Moreover, current physical attacks for object detection struggle to achieve both multi-view effectiveness and visual naturalness in navigation scenarios. To address this, we propose a practical attack method for embodied navigation by attaching adversarial patches to objects, where both opacity and textures are learnable. Specifically, to ensure effectiveness across varying viewpoints, we employ a multi-view optimization strategy based on object-aware sampling, which optimizes the patch’s texture based on feedback from the vision-based perception model used in navigation. To make the patch inconspicuous to human observers, we introduce a two-stage opacity optimization mechanism, in which opacity is fine-tuned after texture optimization. Experimental results demonstrate that our adversarial patches decrease the navigation success rate by an average of 22.39%, outperforming previous methods in practicality, effectiveness, and naturalness. Code is available at: github.com/chen37058/Physical-Attacks-in-Embodied-Nav.

I. INTRODUCTION

Embodied vision navigation [1], [2] refers to an agent moving towards a target object or a designated location in an unseen environment. It is widely applied in safety-critical scenarios, such as aiding individuals with disabilities in finding objects within their homes. The integration of Deep Neural Networks (DNNs) enables embodied navigation agents to leverage vision-based signal processing and sequential decision-making techniques [3], driving significant advancements. However, DNNs are known to be vulnerable to adversarial examples [4], [5], [6], posing security risks for DNN-based embodied navigation systems in real-world deployments. In high-risk scenarios such as assistive robotics, security patrolling, and industrial automation, adversarial attackers could exploit these vulnerabilities to manipulate the agent’s decisions, leading to incorrect path planning, target deviations, or even direct threats to human safety. Therefore, studying adversarial attacks on embodied navigation—particularly 3D physical adversarial attacks—is crucial for identifying adversarial robustness issues and advancing the theoretical and technological foundations of secure navigation systems.

¹School of Intelligent Engineering and Automation, Beijing University of Posts and Telecommunications, Beijing 100876, China.

*Corresponding author.

e-mail: chenmeng@bupt.edu.cn.

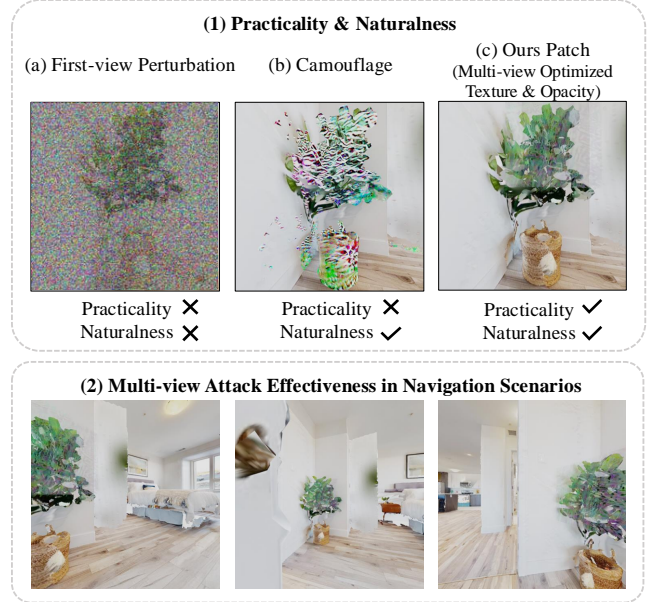


Fig. 1. **Motivation.** Previous attacks were either impractical or failed to achieve both naturalness and multi-view effectiveness in navigation. For instance, prior methods such as (a) applied universal perturbations to first-person views, (b) altered 3D object textures for camouflage. In contrast, our patch (c), with learnable textures and opacity, appears more natural and, as shown in the lower panel (2), effectively prevents detection from multiple viewpoints when placed on the target object.

Recently, research on adversarial attacks against embodied vision navigation has been scarce. For instance, as shown in Figure 1 (a), Ying et al. [7] applied universal perturbations to the agent’s first-person observations. Another approach, as shown in Figure 1 (b), Liu et al. [8] explored 3D adversarial camouflage by perturbing object textures in navigation scenes. Similar object-level texture perturbation attacks targeting object detectors have also been studied in [9], [10], [11], [12], [13]. However, these methods face practical challenges. Applying adversarial stickers directly to the agent’s camera view is impractical, as attackers typically lack control over the agent’s camera. Similarly, modifying object textures and shapes in the scene is costly, often requiring 3D printing, object replacement, or texture projection using projectors.

Other studies on physical adversarial attacks in robotics [14], [15] investigate the placement of small objects in the physical environment to deceive point cloud semantic segmentation in autonomous driving or grasping networks. While these attacks are effective against robots that rely solely on depth sensor information (e.g., point clouds

or depth maps), they remain ineffective against navigation robots that are equipped with only RGB sensors. Several adversarial patch attacks that are physically realizable [16], [17], [18], [19], [20], [21] have been widely applied in areas such as traffic sign detection [17], [22] and facial recognition [23]. These methods typically rely on techniques such as Expectation over Transformation (EoT) [24], [25] to model real-world transformations, including scaling and rotation. However, these methods, including the single-pixel attack proposed in the physical adversarial attack work on robotics [15], are insufficient to effectively address complex viewpoint variations in navigation scenarios. While multi-view adversarial patches [26], [27] are specifically designed to address viewpoint variations, they are primarily developed for adversarial clothing. Their unnatural appearance makes them unsuitable for objects in navigation scenes, as they can be easily noticed by humans. **In summary, existing physical attack methods fail to simultaneously satisfy two key criteria in navigation tasks: (1) Insufficient attack effectiveness under complex viewpoint variations; (2) Lack of naturalness when applied to objects, making them easily detectable and easy to defend against.**

To develop a physically feasible attack method that satisfies both multi-view effectiveness and naturalness in embodied navigation scenarios, we propose attaching an adversarial patch with learnable textures and opacity to navigation target objects. **First, to enhance multi-view attack effectiveness, we employ a multi-view optimization strategy based on object-aware sampling to refine the adversarial patch.** This process selects the most informative viewpoints based on feedback from the navigation vision model. A physics-based differentiable renderer generates first-person images, which are fed into the model to compute detection loss. Gradients then optimize the patch’s texture and opacity. Figure 1 (lower panel) illustrates its effectiveness. **Second, to improve naturalness, we incorporate an opacity optimization mechanism.** The patch comprises an RGB texture and a single-channel opacity mask, both refined via multi-view optimization, ensuring adjustable transparency and minimal perceptibility to human observers.

We conducted experiments on a fundamental embodied navigation task, ObjectNav, using the HM3D scene datasets. We compared our method with prior attack approaches, including full-coverage texture attacks on 3D objects and existing 2D adversarial pixel patches. The results show that our adversarial patches lead to an average reduction of 22.39% in navigation success rates.

The contributions of this research are as follows:

- We propose a physically realizable attack method for embodied vision navigation by attaching adversarial patches with learnable opacity and textures to objects.
- We introduce a multi-view optimization using object-aware sampling to enhance patch effectiveness and opacity optimization for visual naturalness.
- Experimental results show that our adversarial patches outperform previous methods in practicality, effectiveness, and naturalness.

II. RELATED WORK

A. Embodied Vision Navigation.

Embodied navigation [2], [28] involves agents navigating unseen environments using visual inputs. Key tasks include object goal navigation [29], [1], [30], image goal navigation [31], visual language navigation [32], [33], and embodied question answering [34]. Object goal navigation, which requires locating specific object categories in unknown environments, tests scene understanding and memory, with applications like assisting individuals with disabilities. We focus on adversarial attacks in this task, which are fundamental and critical to other embodied tasks.

B. Physical Adversarial Attacks.

Early adversarial attack research on embodied navigation [8] focused on modifying object properties (e.g., 3D shape, texture) in key scene views. Universal perturbations [7] explored patch-based sensor attacks but proved impractical for real-world deployment. Recent work [35] investigates backdoor attacks, where triggers implanted in the training data cause predefined abnormal behaviors in navigation models. This is effective when attackers can distribute compromised models to victims. In contrast, we consider a different threat model: attackers cannot alter the victim’s model but can modify the physical environment, a scenario particularly relevant for protecting key assets in military applications.

Existing studies on physical adversarial attacks on robots [14] use small objects to deceive point cloud segmentation in autonomous driving, which is effective only for depth-based sensors. Similarly, [15] disrupts grasping success with a small sphere but is also limited to depth sensors and fails against navigation robots equipped only with RGB sensors. Moreover, its single-pixel attack struggles with viewpoint variations in navigation.

Several physically realizable adversarial patch attacks [16], [17], [18], [19], [20], [36], [21], [37] have been widely applied in traffic sign detection [17], [22] and facial recognition [23], modify 2D pixel space without altering the object itself. While techniques like Expectation over Transformation (EoT) [24], [25] can simulate real-world transformations (e.g., scaling, rotation), navigation scenarios involve far more diverse and unpredictable viewpoint changes, limiting attack efficacy. Multi-view adversarial patches [26], [27] are mainly designed for clothing, but their unnatural appearance makes them unsuitable for objects in navigation tasks.

To address these limitations, we generate physically realizable adversarial examples for embodied navigation that ensure both multi-view effectiveness and natural appearance in the 3D physical world.

III. METHODOLOGY

In this section, we present our method for generating adversarial patches with learnable textures and opacity, as illustrated in Figure 2.

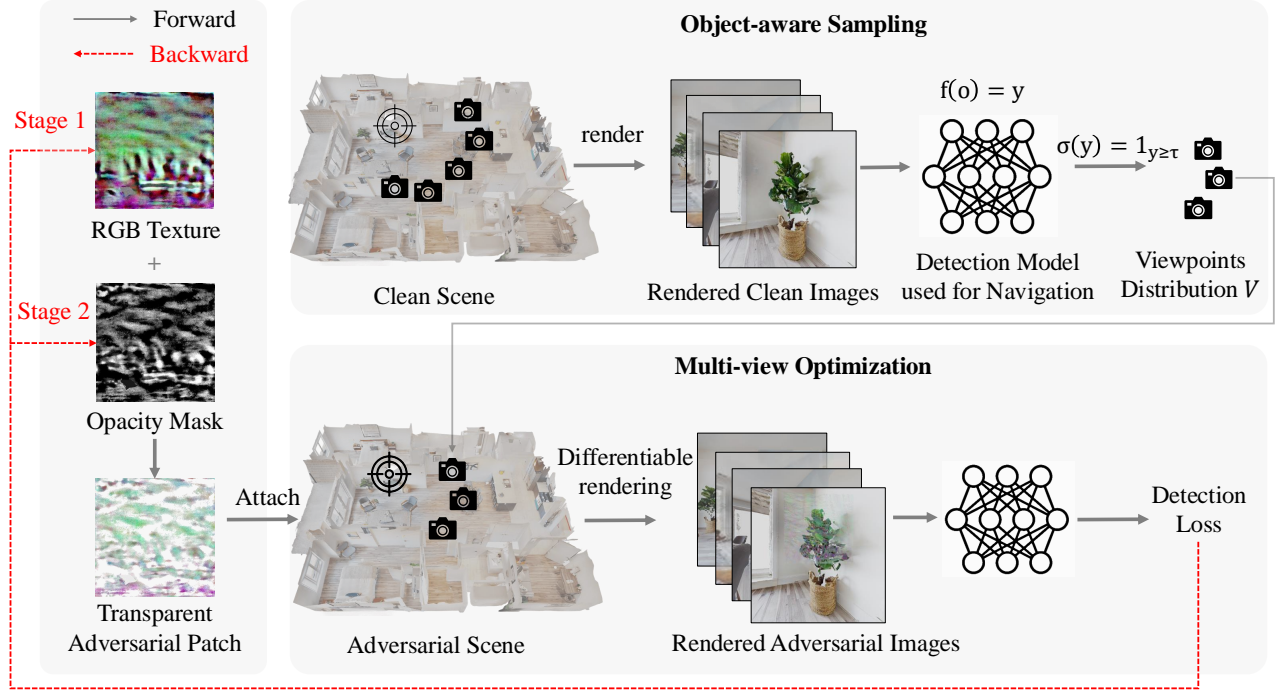


Fig. 2. Method Overview. The initialized patch \mathcal{P}^{adv} is attached to the target object in scene \mathcal{S} . (1) To enhance naturalness, the patch comprises a base texture (three RGB channels) and a single-channel opacity mask, both refined via multi-view optimization (Sec. III-D), enabling adjustable transparency and reducing perceptibility. (2) To ensure multi-view effectiveness, we employ a multi-view optimization strategy based on object-aware sampling. Camera viewpoints are initialized in batches and filtered using the detection/segmentation model f , yielding an optimized viewpoint distribution V (Sec. III-B). (3) We refine the patch using V in multi-view optimization, leveraging a differentiable renderer \mathcal{R} to generate first-person images, which are fed into f to compute detection loss. Gradients are then used to optimize the patch’s texture and opacity via the PGD method (Sec. III-C).

A. Problem Formulation

Given a scenario \mathcal{S} and a detection/segmentation model used for navigation, represented as $f: o \rightarrow y$, our objective is to generate adversarial patches \mathcal{P}^{adv} for target objects in the scene to make these objects undetectable and cause navigation failure. Here, f represents a detection model that identifies objects in the navigation task, o denotes the input image, and y represents the model’s predicted output (e.g., bounding boxes or segmentation masks). The problem is formulated as finding the optimal texture that maximizes the adversarial loss:

$$\max_{\mathcal{P}^{adv}} \left\{ \mathbb{E}_{\mathbf{v} \in V} \mathcal{L}_{attack}[f(\mathcal{R}(\mathcal{S}, \mathcal{P}^{adv}; L, \mathbf{v})), y] \right\}, \quad (1)$$

where $\hat{o} = \mathcal{R}(\mathcal{S}, \mathcal{P}^{adv}; L, \mathbf{v})$ represents the rendered image, L denotes lighting conditions, and \mathbf{v} is the viewpoint from distribution V . \mathcal{L}_{attack} is the loss that induces detection errors in the detection model. The challenge lies in ensuring adversarial robustness across multiple viewpoints. Further details are provided in Sec. III-B and Sec. III-C.

B. Object-aware Sampling

Since target object visibility varies with angles, distances, and scene contexts, we employ a specialized sampling strategy to obtain the most valuable viewpoints for optimizing the patch. We randomly initialize camera viewpoints and filter configurations based on the detection model’s detection

confidence, yielding a distribution V that is optimal for optimization. Cameras are positioned around the target object, and the viewpoint distribution is defined as:

$$\begin{aligned} V &= \{(\mathbf{p}_i(r), \phi_i) \mid r \in R, \sigma(f(o) = 1)\}, \\ i &\in \{0, 1, \dots, N-1\}, \\ \mathbf{p}_i(r) &= \left(c_x + r \cos\left(\frac{2\pi i}{N}\right), c_y, c_z + r \sin\left(\frac{2\pi i}{N}\right) \right), \\ \phi_i &= \left(0, \frac{2\pi i}{N} - \frac{\pi}{2}, \pi \right). \end{aligned} \quad (2)$$

Here, $\mathbf{p}_i(r)$ represents the camera position around the object center (c_x, c_y, c_z) , with radii $r \in R$ ensuring layered coverage. ϕ_i denotes the camera orientation, and N is the number of cameras per circle. The indicator function $\sigma(x) = 1_{x \geq \tau}$ filters configurations based on detection confidence.

C. Multi-view Optimization

To address the challenge of the patch’s multi-view effectiveness, we optimize the patch using a physics-based differentiable renderer and the sampled viewpoint distribution. First-person images from these viewpoints are rendered and fed into the detection model to compute the total detection loss. Gradients from multiple views are used to optimize the patch texture with a gradient-based method. The rendering process is defined as:

$$o = \mathcal{R}(\mathcal{S}; L, \mathbf{p}_i(r), \phi_i), \quad (3)$$

$$\hat{o} = \mathcal{R}(\mathcal{S}, \mathcal{P}^{adv}; L, \mathbf{p}_i(r), \phi_i), \quad (4)$$

where o and \hat{o} are images without and with the adversarial patch, respectively. The final gradient-based update for the patch texture is:

$$\mathcal{P}_{adv} = \mathcal{P}_{adv} + \alpha \cdot \text{sign}(\nabla_{\mathcal{P}_{adv}} L_{\text{total}}(f(\mathcal{R}(\mathcal{S}_{adv}, \mathbf{c})), y)), \quad (5)$$

where α is the learning rate, and $\nabla_{\mathcal{P}_{adv}} L_{\text{total}}$ is the gradient of the total loss with respect to the patch texture. This iterative process ensures robust adversarial patches across multiple viewpoints and lighting conditions.

D. Opacity Optimization

To improve the naturalness of the patch, we incorporate an opacity optimization mechanism. Digitally, our adversarial patch consists of a base texture image with three RGB color channels and a single-channel opacity mask, where transparency values range from 0 to 255, with 255 representing full opacity and 0 representing full transparency. Both the base texture and the opacity mask are optimized for effectiveness. Intuitively, we consider the primary role of the texture to be enhancing the attack’s efficacy, while the opacity mainly serves to reduce the patch’s visibility to the human eye. Thus, as shown in Figure 3, we employ a two-stage optimization strategy. In the first stage, we randomly initialize a three-channel RGB texture and a constant single-channel opacity mask, combining them to form the initial adversarial patch. This patch is iteratively optimized using the strategies described in Section III-B and Section III-C, resulting in an effective adversarial texture. In the second stage, we optimize the opacity mask based on the optimized texture, using the same optimization approach. All optimizations are conducted using a gradient-based PGD (Projected Gradient Descent) method.

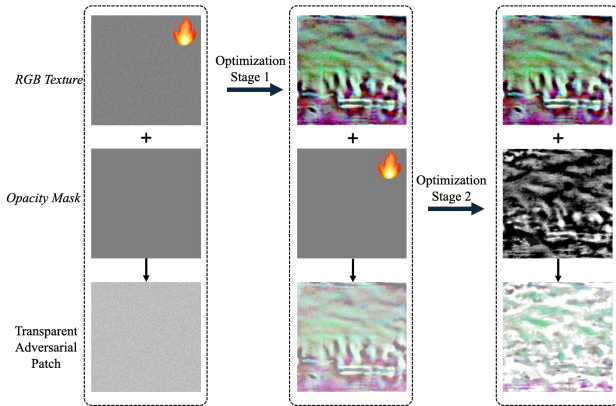


Fig. 3. **Opacity Optimization Strategy.** The first stage optimizes the RGB texture to enhance the attack’s efficacy, while the second stage refines the opacity mask to reduce the patch’s detectability to the human eye.

Physically, this transparency image can be printed on transparent paper using a laser printer and then directly

TABLE I
ATTACK PERFORMANCE AGAINST MULTIPLE TARGETS IN HM3D FOR NAVIGATION

Target	Attack Method	SR↓(%)	SPL↓(%)	DTS↑(m)
tv monitor	No Attack	100.00	63.03	0.04
	Camouflage	100.00(0.00↓)	56.37(6.66↓)	0.04(0.00↑)
	Ours Patch	60.00 (40.00↓)	14.81 (48.22↓)	1.68 (1.64↑)
plant	No Attack	93.75	26.60	0.24
	Camouflage	37.50 (56.25↓)	11.87(14.73↓)	1.06 (0.82↑)
	Ours Patch	62.50 (31.25↓)	7.98 (18.62↓)	0.73(0.49↑)
bed	No Attack	94.11	55.83	0.16
	Camouflage	94.11(0.00↓)	55.95(0.12↓)	0.16(0.00↑)
	Ours Patch	94.11 (0.00↓)	46.44 (9.39↓)	0.16 (0.00↑)
chair	No Attack	100.00	65.18	0.22
	Camouflage	100.00(0.00↓)	58.97(6.21↓)	0.22(0.00↑)
	Ours Patch	83.33 (16.67↓)	47.12 (18.06↓)	0.34 (0.12↑)
sofa	No Attack	100.00	57.28	0.36
	Camouflage	100.00(0.00↓)	50.45(6.83↓)	0.36(0.00↑)
	Ours Patch	78.57 (21.43↓)	42.19 (15.09↓)	0.52 (0.16↑)
toilet	No Attack	81.25	43.32	1.32
	Camouflage	75.00(6.25↓)	36.85(6.47↓)	1.49(0.17↑)
	Ours Patch	56.25 (25.00↓)	27.42 (15.90↓)	1.93 (0.61↑)
Average	No Attack	94.85	51.87	0.39
	Camouflage	84.44(10.41↓)	45.08(6.79↓)	0.56(0.17↑)
	Ours Patch	72.46 (22.39↓)	30.99 (20.88↓)	0.89 (0.50↑)

affixed to the target object. This approach is particularly practical in navigation scenarios, as it eliminates the need to modify the properties of existing scene objects. Moreover, the patch’s adjustable transparency ensures it remains inconspicuous to human observers.

IV. EXPERIMENTS

A. Experimental Setup

Settings. We use the modular-based navigation agent from [38] for ObjectNav, which incorporates a Mask R-CNN [39] for object instance segmentation. Our navigation experiment setup follows the 2022 Habitat ObjectNav Challenge [40]. For the adversarial attack, we conduct experiments in ObjectNav using the HM3D dataset [41] within the Habitat simulator [42], [43]. We perform white-box optimization using scenes from the validation dataset, with attack targets being several categories listed in Table I. A 512×512 adversarial patch with four RGBA channels is used, initialized with Gaussian noise and manually positioned on the target object. Mitsuba 3 [44] serves as the renderer, using planar area lights or “constant” scene lighting with an intensity parameter of 40., and a camera resolution of 512×512 . During texture and opacity optimization, the detection confidence threshold is set to 0.5. We apply PGD attacks over 100 iterations with a step size of 1.

Evaluations. We evaluate attack performance using three metrics from [38]: Success Rate (SR), Success weighted by Path Length (SPL), and Distance to Goal (DTS). SR measures the agent’s ability to successfully locate the target object, while SPL considers both the success rate and the efficiency of the path taken. DTS quantifies the remaining distance between the agent and the goal at the end of each episode. Additionally, we measure the Attack Success Rate

TABLE II
ATTACK PERFORMANCE ON MULTI-VIEW OBJECT DETECTION.

Attack Method	ASR \uparrow (%)
No Attack	19.01
Camouflage [8]	85.12(66.11 \uparrow)
Adversarial Patch (Random Texture)	29.75(10.74 \uparrow)
Adversarial Patch (2D Optimized Texture)	74.38(55.37 \uparrow)
<i>Ours</i> Patch (Multi-view Optimized Texture)	89.26 (70.25 \uparrow)
<i>Ours</i> Patch (Multi-view Optimized Texture & Opacity)	98.35 (79.34\uparrow)

(ASR), which is defined as the proportion of viewpoints that were successfully attacked (i.e., viewpoints where detection fails) among all sampled viewpoints.

B. Attack Performance

Table I shows the attack performance of our adversarial patch, which underwent multi-view optimization and opacity optimization, in the navigation task. Since camouflage [8] is the only physically realizable adversarial attack method specifically designed for embodied navigation, we limited our comparison to this method. Our method significantly reduces the agent’s success rate (SR) across multiple target categories, with an average reduction of 22.39%. Specifically, it achieves a 40.00% decrease in SR for TV monitors, 31.25% for plants, and 25.00% for toilets. Additionally, our approach leads to a substantial drop in SPL, demonstrating that even when the agent succeeds, it takes a much less efficient path. Moreover, the distance to goal (DTS) consistently increases, indicating greater difficulty in reaching the intended target. The visualization in Figure 4 further illustrates the superior attack performance compared to the baseline 3D camouflage method. Figure 5 illustrates that our adversarial patch exhibits greater visual naturalness.

Table II further presents the Attack Success Rate (ASR) for multi-view target detection in a navigation scenario.

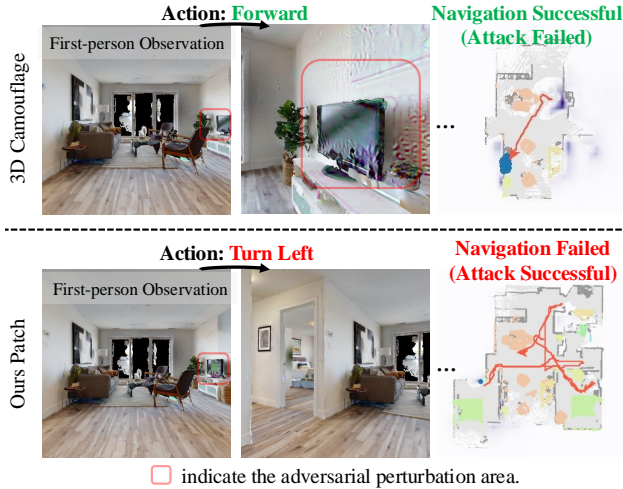


Fig. 4. **Visualization of the attack performance of our adversarial patch compared to 3D camouflage in the navigation task.** The first row shows the adversarial scenario with 3D camouflage, where the agent was still able to successfully navigate and locate the target. In contrast, in the scenario with our adversarial patch, the agent failed to detect the target even after 499 steps, resulting in navigation failure.

In this experiment, we applied our object-aware sampling strategy to sample viewpoints around the television monitor, obtaining a total of 120 viewpoints. Specifically, 20 viewpoints were used to optimize the full-coverage texture or adversarial patch, while the remaining 100 unseen viewpoints were reserved for testing. ASR is defined as the percentage of these 100 unseen viewpoints in which the attack succeeded (i.e., detection failed, with a confidence threshold of 0.5). We compared our method with prior physically realizable approaches, including camouflage [8]. Additionally, we considered 2D-optimized texture patches without differentiable rendering and multi-view optimization [16], [17], [18], [19], [20], [21], as well as adversarial patches with randomly initialized textures. Our experiments demonstrate that the proposed multi-view sampling strategy achieved an ASR of 89.26% in a small-sample experiment with 100 viewpoints around the television. By incorporating opacity optimization, ASR was further improved, reaching up to 98.35%, surpassing the baseline performance.

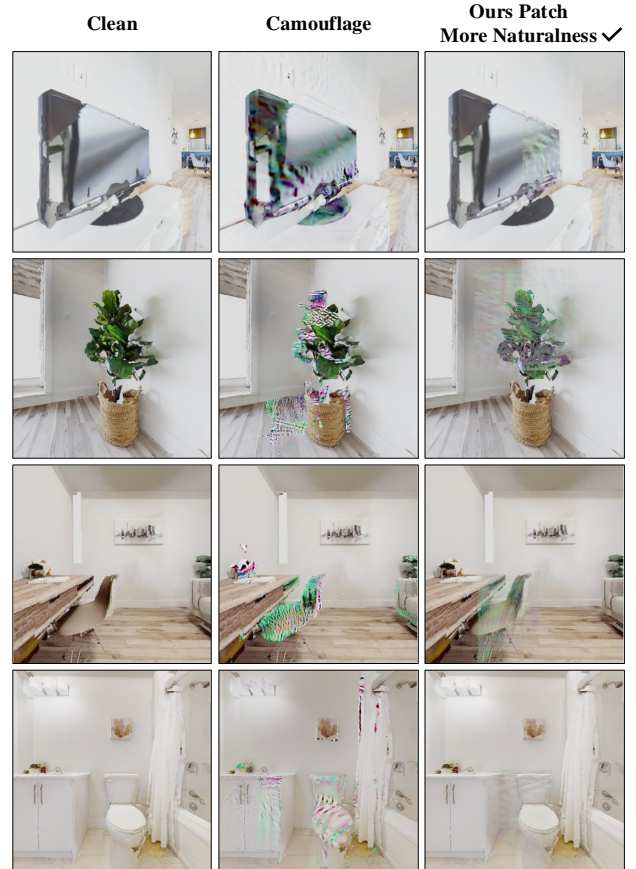


Fig. 5. **Comparison of naturalness.** From left to right, the images show the previous camouflage method, our adversarial patch, and the clean scene. Our adversarial patch exhibits greater visual naturalness.

C. Ablation Study

In this section, we conduct ablation experiments to investigate the impact of two components: the multi-view optimization strategy based on object-aware sampling and the opacity optimization strategy. The objective is to provide insights into the key factors driving performance improvements.

TABLE III
ABLATION STUDY ON ATTACK COMPONENTS.

Texture Optimization	Opacity Optimization	Viewpoints	ASR↑(%)
×	×	-	28.93
✓	×	1	73.55(44.62↑)
✓	×	20	89.26(60.33↑)
✓	✓	20	99.17(70.24↑)

Effect of multi-view optimization based on object-aware sampling. The experimental results are shown in Table III. As observed, when neither multi-view texture optimization nor opacity optimization is applied, the ASR is the lowest at 28.93%. When only single-view texture optimization is applied, there is an improvement, and multi-view texture optimization leads to even higher performance. When both texture and opacity are optimized, the ASR reaches its highest value of 99.17%, validating the effectiveness of our multi-view optimization strategy.

Effect of opacity optimization. As shown in Figure 6, after applying opacity optimization, we observe that the patch appears significantly more natural. In addition, we studied the effect of different initial opacity levels, as shown in Table IV. We applied varying levels of opacity to both randomly initialized and optimized textures. At an opacity of 0.2, the patch is nearly invisible, while at 0.8, it is nearly opaque. Higher opacity typically results in a higher ASR but also makes the patch more noticeable. In our quantitative experiments, we selected an initial opacity of 0.6 for both texture and opacity optimization, as it provides a balance between attack effectiveness and visibility, and then optimized the opacity mask parameters based on this initial setting. Finally, Figure 7 presents the rendered effects of the adversarial patch with opacity using various renderers.

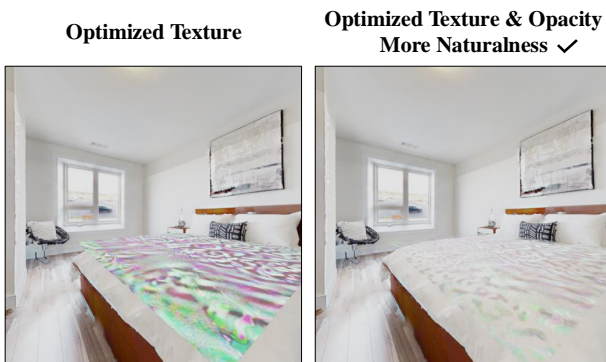


Fig. 6. **Visualization of the effect of opacity optimization.** It is evident that after applying opacity optimization, the naturalness of the patch improves significantly.

V. CONCLUSIONS

In this paper, We propose a practical attack on embodied navigation using adversarial patches with learnable textures and opacity on objects, reducing success rates by 22.39% on

TABLE IV
ABLATION STUDY ON OPACITY VALUE.

Method	Opacity Value(%)	ASR↑(%)
Texture Random	0.20	24.79
	0.40	21.49
	0.60	15.70
	0.80	29.75
Texture Optimized	0.20	22.31
	0.40	71.90
	0.60	90.91
	0.80	87.60

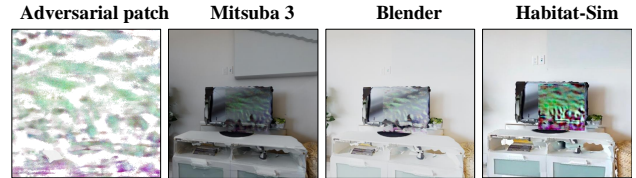


Fig. 7. **Visualization of adversarial patches with opacity under different renderers.** Due to differences in physical rendering techniques and lighting setups, this highlights the challenge of ensuring cross-renderer transferability and maintaining attack effectiveness. Notably, the habitat-sim renderer lacks support for transparent materials, making the texture appear more visible in its renderings.

average. While our method demonstrates strong performance in simulation, further research is needed to develop effective printing techniques for patches with optimized opacity. Additionally, their perceptibility to human observers should be assessed in real-world settings. Although real-world experiments were not conducted, our work significantly improves upon prior approaches—including first-person universal perturbations, full-coverage 3D textures, and ineffective multi-view adversarial patches. It achieves notable advancements in physical feasibility, multi-view attack effectiveness, and visual naturalness. Moreover, virtual 3D environments remain an essential part of future embodied navigation research.

ACKNOWLEDGMENT

This work was supported by the National Natural Science Foundation of China (Grant No. 62173045), the Beijing Natural Science Foundation under Grant F2024203115, the China Postdoctoral Science Foundation under Grant Number 2024M750255, and the “Double First-Class” Interdisciplinary Team Project of Beijing University of Posts and Telecommunications under Grant 2023SYLTD02.

REFERENCES

- [1] D. S. Chaplot, D. Gandhi, A. Gupta, and R. Salakhutdinov, “Object goal navigation using goal-oriented semantic exploration,” in *Proceedings of the Neural Information Processing Systems (NeurIPS)*, 2020.
- [2] H. Wang, W. Liang, L. Van Gool, and W. Wang, “Towards versatile embodied navigation,” in *Proceedings of the Neural Information Processing Systems (NeurIPS)*, 2022.
- [3] F. Zhu, Y. Zhu, V. Lee, X. Liang, and X. Chang, “Deep learning for embodied vision navigation: A survey,” *arXiv Preprint arXiv:2108.04097*, 2021.
- [4] I. J. Goodfellow, J. Shlens, and C. Szegedy, “Explaining and harnessing adversarial examples,” *arXiv Preprint arXiv:1412.6572*, 2014.

- [5] N. Carlini and D. Wagner, "Towards evaluating the robustness of neural networks," in *Proceedings of the IEEE Symposium on Security and Privacy (S&P)*, 2017, pp. 39–57.
- [6] C. Xiao, B. Li, J.-Y. Zhu, W. He, M. Liu, and D. Song, "Generating adversarial examples with adversarial networks," *arXiv Preprint arXiv:1801.02610*, 2018.
- [7] C. Ying, Y. Qiaoben, X. Zhou, H. Su, W. Ding, and J. Ai, "Consistent attack: Universal adversarial perturbation on embodied vision navigation," *Pattern Recognition Letters*, pp. 57–63, 2023.
- [8] A. Liu, T. Huang, X. Liu, Y. Xu, Y. Ma, X. Chen, S. J. Maybank, and D. Tao, "Spatiotemporal attacks for embodied agents," in *Proceedings of the European Conference on Computer Vision (ECCV)*, 2020, pp. 122–138.
- [9] Y. Huang, Y. Dong, S. Ruan, X. Yang, H. Su, and X. Wei, "Towards transferable targeted 3d adversarial attack in the physical world," in *Proceedings of the IEEE/CVF Conference on Computer Vision and Pattern Recognition (CVPR)*, 2024, pp. 24 512–24 522.
- [10] N. Suryanto, Y. Kim, H. T. Larasati, H. Kang, T.-T.-H. Le, Y. Hong, H. Yang, S.-Y. Oh, and H. Kim, "Active: Towards highly transferable 3d physical camouflage for universal and robust vehicle evasion," in *Proceedings of the IEEE/CVF International Conference on Computer Vision (ICCV)*, 2023, pp. 4305–4314.
- [11] N. Suryanto, Y. Kim, H. Kang, H. T. Larasati, Y. Yun, T.-T.-H. Le, H. Yang, S.-Y. Oh, and H. Kim, "Dta: Physical camouflage attacks using differentiable transformation network," in *Proceedings of the IEEE/CVF Conference on Computer Vision and Pattern Recognition (CVPR)*, 2022, pp. 15 305–15 314.
- [12] D. Wang, T. Jiang, J. Sun, W. Zhou, Z. Gong, X. Zhang, W. Yao, and X. Chen, "Fca: Learning a 3d full-coverage vehicle camouflage for multi-view physical adversarial attack," in *Proceedings of the AAAI Conference on Artificial Intelligence (AAAI)*, 2022, pp. 2414–2422.
- [13] J. Wang, A. Liu, Z. Yin, S. Liu, S. Tang, and X. Liu, "Dual attention suppression attack: Generate adversarial camouflage in physical world," in *Proceedings of the IEEE/CVF Conference on Computer Vision and Pattern Recognition (CVPR)*, 2021, pp. 8565–8574.
- [14] Y. Zhu, C. Miao, F. Hajiaghajani, M. Huai, L. Su, and C. Qiao, "Adversarial attacks against lidar semantic segmentation in autonomous driving," in *Proceedings of the ACM Conference on Embedded Networked Sensor Systems (SenSys)*, 2021, pp. 329–342.
- [15] N. W. Alharthi and M. Brandão, "Physical and digital adversarial attacks on grasp quality networks," in *Proceedings of the IEEE International Conference on Robotics and Automation (ICRA)*, 2024, pp. 1907–1902.
- [16] T. B. Brown, D. Mané, A. Roy, M. Abadi, and J. Gilmer, "Adversarial patch," *arXiv Preprint arXiv:1712.09665*, 2017.
- [17] K. Eykholt, I. Evtimov, E. Fernandes, B. Li, A. Rahmati, C. Xiao, A. Prakash, T. Kohno, and D. Song, "Robust physical-world attacks on deep learning visual classification," in *Proceedings of the IEEE/CVF Conference on Computer Vision and Pattern Recognition (CVPR)*, 2018, pp. 1625–1634.
- [18] C. Yang, A. Kortylewski, C. Xie, Y. Cao, and A. Yuille, "Patchattack: A black-box texture-based attack with reinforcement learning," in *Proceedings of the European Conference on Computer Vision (ECCV)*, 2020, pp. 681–698.
- [19] X. Liu, H. Yang, Z. Liu, L. Song, H. Li, and Y. Chen, "Dpatch: An adversarial patch attack on object detectors," *arXiv Preprint arXiv:1806.02299*, 2018.
- [20] X. Yang, Y. Dong, T. Pang, Z. Xiao, H. Su, and J. Zhu, "Controlable evaluation and generation of physical adversarial patch on face recognition," *arXiv Preprint arXiv:2203.04623*, 2022.
- [21] C. Kang, Y. Dong, Z. Wang, S. Ruan, Y. Chen, H. Su, and X. Wei, "Diffender: Diffusion-based adversarial defense against patch attacks," in *Proceedings of the European Conference on Computer Vision (ECCV)*, 2024, pp. 130–147.
- [22] X. Wei, Y. Guo, J. Yu, and B. Zhang, "Simultaneously optimizing perturbations and positions for black-box adversarial patch attacks," *IEEE Transactions on Pattern Analysis and Machine Intelligence (TPAMI)*, 2022.
- [23] M. Sharif, S. Bhagavatula, L. Bauer, and M. K. Reiter, "Accessorize to a crime: Real and stealthy attacks on state-of-the-art face recognition," in *Proceedings of the ACM SIGSAC Conference on Computer and Communications Security (CCS)*, 2016, pp. 1528–1540.
- [24] A. Athalye, L. Engstrom, A. Ilyas, and K. Kwok, "Synthesizing robust adversarial examples," in *Proceedings of the International Conference on Machine Learning (ICML)*, 2018, pp. 284–293.
- [25] R. R. Wiyatno and A. Xu, "Physical adversarial textures that fool visual object tracking," in *Proceedings of the IEEE/CVF International Conference on Computer Vision (ICCV)*, 2019, pp. 4822–4831.
- [26] S. Oslund, C. Washington, A. So, T. Chen, and H. Ji, "Multiview robust adversarial stickers for arbitrary objects in the physical world," *Journal of Computational and Cognitive Engineering*, pp. 152–158, 2022.
- [27] Z. Hu, W. Chu, X. Zhu, H. Zhang, B. Zhang, and X. Hu, "Physically realizable natural-looking clothing textures evade person detectors via 3d modeling," in *Proceedings of the IEEE/CVF Conference on Computer Vision and Pattern Recognition (CVPR)*, 2023, pp. 16 975–16 984.
- [28] T. Gervet, S. Chintala, D. Batra, J. Malik, and D. S. Chaplot, "Navigating to objects in the real world," *Science Robotics*, p. eadf6991, 2023.
- [29] H. Du, X. Yu, and L. Zheng, "Vtnet: Visual transformer network for object goal navigation," *arXiv Preprint arXiv:2105.09447*, 2021.
- [30] A. Majumdar, G. Aggarwal, B. Devnani, J. Hoffman, and D. Batra, "Zson: Zero-shot object-goal navigation using multimodal goal embeddings," in *Proceedings of the Neural Information Processing Systems (NeurIPS)*, 2022.
- [31] N. Kim, O. Kwon, H. Yoo, Y. Choi, J. Park, and S. Oh, "Topological semantic graph memory for image-goal navigation," in *Proceedings of the Conference on Robot Learning (CoRL)*, 2023, pp. 393–402.
- [32] S.-M. Park and Y.-G. Kim, "Visual language navigation: A survey and open challenges," *Artificial Intelligence Review*, pp. 365–427, 2023.
- [33] J. Krantz, E. Wijmans, A. Majumdar, D. Batra, and S. Lee, "Beyond the nav-graph: Vision-and-language navigation in continuous environments," in *Proceedings of the European Conference on Computer Vision (ECCV)*, 2020, pp. 104–120.
- [34] A. Das, S. Datta, G. Gkioxari, S. Lee, D. Parikh, and D. Batra, "Embodied question answering," in *Proceedings of the IEEE/CVF Conference on Computer Vision and Pattern Recognition (CVPR)*, 2018, pp. 1–10.
- [35] K. He, K. Chen, J. Bai, Y. Huang, Q. Wu, S.-T. Xia, and L. Wang, "Everyday object meets vision-and-language navigation agent via backdoor," in *Proceedings of the Neural Information Processing Systems (NeurIPS)*, 2024.
- [36] X. Wei, S. Ruan, Y. Dong, and H. Su, "Distributional modeling for location-aware adversarial patches," *arXiv Preprint arXiv:2306.16131*, 2023.
- [37] Z. Xiao, X. Gao, C. Fu, Y. Dong, W. Gao, X. Zhang, J. Zhou, and J. Zhu, "Improving transferability of adversarial patches on face recognition with generative models," in *Proceedings of the IEEE/CVF Conference on Computer Vision and Pattern Recognition (CVPR)*, 2021, pp. 11 845–11 854.
- [38] A. J. Zhai and S. Wang, "Peanut: Predicting and navigating to unseen targets," in *Proceedings of the IEEE/CVF International Conference on Computer Vision (ICCV)*, 2023, pp. 10 926–10 935.
- [39] K. He, G. Gkioxari, P. Dollár, and R. Girshick, "Mask r-cnn," in *Proceedings of the IEEE/CVF International Conference on Computer Vision (ICCV)*, 2017, pp. 2961–2969.
- [40] K. Yadav, J. Krantz, R. Ramakrishna, S. K. Ramakrishnan, J. Yang, A. Wang, J. Turner, A. Gokaslan, V.-P. Berges, R. Mottaghi, O. Maksymets, A. X. Chang, M. Savva, A. Clegg, D. S. Chaplot, and D. Batra, "Habitat challenge 2023," 2023.
- [41] S. K. Ramakrishnan, A. Gokaslan, E. Wijmans, O. Maksymets, A. Clegg, J. M. Turner, E. Undersander, W. Galuba, A. Westbury, A. X. Chang, M. Savva, Y. Zhao, and D. Batra, "Habitat-matterport 3d dataset (hm3d): 1000 large-scale 3d environments for embodied ai," in *Proceedings of the Neural Information Processing Systems Datasets and Benchmarks Track (NeurIPS)*, 2021.
- [42] M. Savva, A. Kadian, O. Maksymets, Y. Zhao, E. Wijmans, B. Jain, J. Straub, J. Liu, V. Koltun, J. Malik, D. Parikh, and D. Batra, "Habitat: A platform for embodied ai research," in *Proceedings of the IEEE/CVF International Conference on Computer Vision (ICCV)*, 2019.
- [43] A. Szot, A. Clegg, E. Undersander, E. Wijmans, Y. Zhao, J. Turner, N. Maestre, M. Mukadam, D. Chaplot, O. Maksymets, A. Gokaslan, V. Vondrus, S. Dharur, F. Meier, W. Galuba, A. Chang, Z. Kira, V. Koltun, J. Malik, M. Savva, and D. Batra, "Habitat 2.0: Training home assistants to rearrange their habitat," in *Proceedings of the Neural Information Processing Systems (NeurIPS)*, 2021.
- [44] W. Jakob, S. Speierer, N. Roussel, and D. Vicini, "Dr.jit: A just-in-time compiler for differentiable rendering," *Transactions on Graphics (SIGGRAPH)*, 2022.